Sequence-Specific ^1H, ^{13}C, and ^{15}N NMR Assignments for Oxidized Ferredoxin from *Clostridium pasteurianum*

Sergio D. B. Scrofani,*,† Robert T. C. Brownlee,‡ Maruse Sadek,*,‡ and Anthony G. Wedd†

School of Chemistry, University of Melbourne, Parkville, Victoria 3052, Australia, and School of Chemistry, La Trobe University, Bundoora 3083, Australia

Received February 3, 1995[⊗]

Sequence-specific ^{13}C and ^{15}N NMR assignments for the oxidized form of the $2[Fe_4S_4]^{2+}$ ferredoxin from *Clostridium pasteurianum* are presented. Partial or complete sequence-specific ^1H NMR assignments for 52 of the 55 amino acid residues are also derived, extending those previously identified in this paramagnetic protein (Gaillard J.; Moulis, J.-M.; Kümmerle, R.; Meyer, J. *Magn. Reson. Chem.* **1993**, *31*, S27). Protons which remain unassigned are in regions close to the paramagnetic clusters. The ^1H resonances for all but nine non-cysteinyl amide groups have been assigned specifically. Those which have not been assigned are all likely NH···S donors to either a cluster sulfide or cysteinyl S^γ. Eight of the nine are symmetry-related (V9/I38, G12/G41, A13/N42 and A22/A51). Eight paramagnetically shifted non-proline ^{15}N resonances (140−170 ppm) exhibit a pairwise arrangement in two-dimensional ^{15}N acquired INEPT experiments. The NH functions of symmetry-related residues Cys 47 and Cys 18 have been assigned specifically. Assignments for the NH functions for symmetry-related residues Cys 14 and Cys 43 are made on the basis of their close proximity to the paramagnetic centers.

Introduction

At first sight, paramagnetic metalloproteins do not appear to be suitable candidates for structural determination by NMR[1] methods, since the effects of paramagnetically-induced relaxation for nuclei close to paramagnetic centers cannot be predicted easily.[2] Although recent ^1H NMR studies on iron−sulfur proteins have been very useful in defining domains well-removed from these centers,[3−9] information on regions close to the metal sites has been difficult to obtain. This is due to the increased proton relaxation rates induced by the paramagnetic centers. For similar reasons, NOE information in these regions is greatly attenuated.[2] Studies of oxidized plant ferredoxins failed to detect resonances of protons sited less than 7.8 Å from an iron atom of the $[Fe_2S_2]^{2+}$.[5,6,8] In contrast, many of the backbone amide proton resonances located less than 6.5 Å from an iron atom in the single $[Fe_4S_4]^{2+}$ cluster of reduced HiPIPs are identified.[7,10] This difference in distance threshold is apparently controlled by variations in the relaxation processes induced by the two different clusters. There are two $[Fe_4S_4]^{2+}$ clusters in oxidized ferredoxin from *Clostridium pasteurianum* (*Cp*Fd), complicating the situation further. The residual paramagnetism present at room temperature ($\mu_{eff} \sim 2\ \mu_B$ per cluster[11]) is responsible for dramatic differences in chemical shifts and for increased line widths for resonances of nuclei close to paramagnetic centers compared to values observed in diamagnetic proteins.[12,13]

The iron atoms in each of the two Fe−S clusters in *Cp*Fd are linked to the protein backbone through cysteinyl thiolate ligands (Figure 1).[14,15] Together with orientation of peptide amide groups and access to solvent water, NH···S hydrogen bonding involving the sulfur atoms of the Fe−S clusters and their cysteinyl ligands modulate both redox potentials and electron transfer pathways in such proteins.[15−17]

Our aim is to define the structure of *Cp*Fd using NMR methods to assist identification and study of sites involved in electron transfer with redox partners. We detail here a multinuclear NMR study of *Cp*Fd employing both native and ^{15}N labeled protein.

Studies of the $[Fe_2S_2]^{2+}$ vegetative ferredoxin from *Anabaena 7120* have revealed resonances with shifts of up to 310 ppm in

† University of Melbourne.
‡ La Trobe University.
⊗ Abstract published in *Advance ACS Abstracts,* June 15, 1995.

(1) Abbreviations: *Cau*Fd, ferredoxin from *Clostridium acidi-urici*; *Cp*, *Clostridium pasteurianum*; *Cp*Fd, ferredoxin from *C. pasteurianum*; CSI, chemical shift index; DQ−COSY, double-quantum correlation spectroscopy; DQF−COSY, double-quantum filtered correlation spectroscopy; DSS, sodium 2,2-dimethyl-2-silapentane-5-sulfonate; Fe−S, iron−sulfur; HiPIP, high potential iron protein; HMQC, heteronuclear multiple-quantum coherence; HSQC, heteronuclear single-quantum coherence; INEPT, insensitive nuclei enhanced by polarization transfer; NMR, nuclear magnetic resonance; NOE, nuclear Overhauser effect; NOESY, nuclear Overhauser spectroscopy; *Pa*Fd, ferredoxin from *Peptococcus aerogenes*; ROESY, rotating frame Overhauser spectroscopy; TOCSY, total correlation spectroscopy; TPPI, time proportional phase incrementation.

(2) La Mar, G. N.; de Ropp, J. S. In *Biological Magnetic Resonance, Volume 12: NMR of Paramagnetic Molecules;* Berliner, L. J., Reuben, J., Eds.; Plenum Press: New York, 1993.
(3) Oh, B.-H.; Markley, J. L. *Biochemistry* **1990**, *29*, 3993.
(4) Oh, B.-H.; Markley, J. L. *Biochemistry* **1990**, *29*, 4004.
(5) Oh, B.-H.; Markley, J. L. *Biochemistry* **1990**, *29*, 4012.
(6) Ye, X. M.; Pochapsky, T. C.; Pochapsky, S. S. *Biochemistry* **1992**, *31*, 1961.
(7) Gaillard, J.; Albrand, J.-P. Moulis, J.-M.; Wemmer, D. E. *Biochemistry* **1992**, *31*, 5632.
(8) Chae, Y. K.; Abildgaard, F.; Mooberry, E. S.; Markley, J. L. *Biochemistry* **1994**, *33*, 3278.
(9) Teng, Q.; Zhour, Z. H.; Smith, E. T.; Busse, S. C.; Howard, J. B.; Adams, M. W. W.; La Mar, G. N. *Biochemistry* **1994**, *33*, 6316.
(10) Bertini, I.; Felli, I. C.; Kastrau, D. H. W.; Luchinat, C.; Piccioli, M. *Eur. J. Biochem.* **1994**, *225*, 703.
(11) Gaillard, J.; Moulis, J.-M.; Meyer, J. *Inorg. Chem.* **1987**, *26*, 320.
(12) Bertini, I.; Capozzi, F.; Luchinat, C.; Piccioli, M.; Vila, A. J. *J. Am. Chem. Soc.* **1994**, *116*, 651.
(13) Scrofani, S. D. B.; Brereton, P. S.; Hamer, A. M.; Lavery, M. J.; McDowell, S. G.; Vincent, G. A.; Brownlee, R. T. C.; Hoogenraad, N. J.; Sadek, M.; Wedd, A. G. *Biochemistry* **1994**, *33*, 14486.
(14) Adman, E. T.; Sieker, L. C.; Jensen, L. H. *J. Biol Chem.* **1973**, *248*, 3987.
(15) Backes, G.; Mino, Y.; Loehr, T. M.; Meyer, T. E.; Cusanovich, M. A.; Sweeney, W. V.; Adman, E. T.; Sanders-Loehr, J. *J. Am. Chem. Soc.* **1991**, *113*, 2055.
(16) Jensen, G. M.; Warshel, A.; Stephens, P. J. *Biochemistry* **1994**, *33*, 10911.
(17) Ueyama, N.; Okamura, T.; Nakamura, A. *J. Chem. Soc., Chem. Commun.* **1992**, 1019.

0020-1669/95/1334-3942$09.00/0

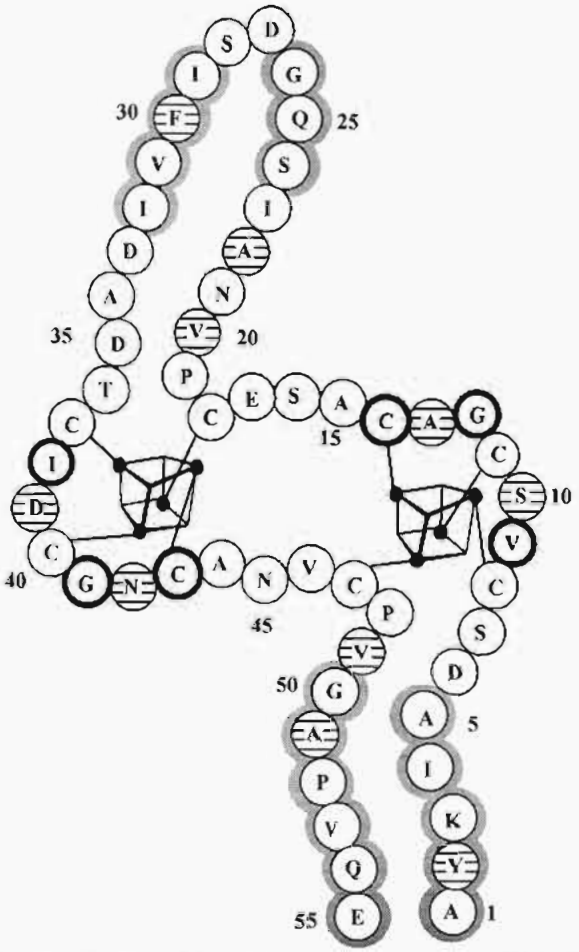

Figure 1. Simple two-dimensional representation of *Cp*Fd. NMR data predicts that the shaded residues participate in β-sheet structure. The crystal structure of *Pa*Fd[15] predicts that residues outlined in bold will be likely NH hydrogen bond donors to cluster sulfides, while circles with horizontal lines represent residues which are NH···S donors to cysteinyl thiolates. Although not discussed specifically,[15] Cys 11 and Cys 40 are likely NH···S donors to cluster sulfides.

^{1}H-decoupled ^{15}N spectra, with line widths greater than 400 Hz.[5] However, due to its lower magnetogyric ratio, such paramagnetic effects are not as dramatic for ^{15}N as they are for ^{1}H or ^{13}C nuclei in similar environments.[18] In the present work, the advantages of acquiring NMR data through ^{15}N nuclei has been exploited, allowing all NH functions in *Cp*Fd to be identified. A preliminary report has been communicated.[19]

Specifically designed mutant forms of *Cp*Fd have been prepared to assist in identification of regions closer to the paramagnetic centers.[13] In addition, a structural model of *Cp*Fd[13] has been derived from the crystal structure of the 2[Fe_4S_4]$^{2+}$ ferredoxin from *Peptococcus aerogenes* (*Pa*Fd; 70% homology)[15] to assist interpretation of the structural information obtained from NMR results. Sequence-specific ^{1}H NMR assignments of *Cp*Fd are presented here which confirm and extend assignments presented by Gaillard and co-workers.[20] A comprehensive list of $^3J_{NH\alpha}$ vicinal coupling constants, amide proton exchange rates, and observed sequential and long-range NOE connectivities are described. These results allow development of a more detailed view of the secondary structure of *Cp*Fd.

Experimental Section

Bacterial Growth and Isolation. Growth of native *C. pasteurianum* (*Cp*) was initiated by inoculating 20 mL cultures containing dehydrated minced beef (5 g), Schaedler's anaerobic broth (25.6 g L^{-1}, Oxoid Co.) and glucose (5 g L^{-1}), with a single colony from a freshly streaked plate. The seed colony was grown until late log phase at 37 °C and subsequently used to inoculate a 16 L culture[21] purged with high purity argon gas. For ^{15}N labeled cultures, $(^{15}NH_4)_2SO_4$ (1.5 g L^{-1}) was the sole ^{15}N source and the $CaCO_3$ content was doubled (2 g L^{-1}). All cultures were harvested at an OD_{660} of approximately 3, yielding about 110 g of wet cells. The isolation of wild-type *Cp*Fd has been described previously.[21] Preparation of recombinant and Gly to Ala mutant forms of *Cp*Fd are as described previously.[13] Preparation of the Asp 39 to Asn (D39N) mutant will be described elsewhere.[22] Deuteration of protein samples was performed by first exchanging buffer in an Amicon ultrafiltration cell equipped with a YM3 membrane, and then an Amicon Centricon 3 microconcentrator. All samples were degassed and sealed under an atmosphere of dinitrogen gas.

NMR Experimental Data. NMR spectra were recorded on oxidized *Cp*Fd dissolved in 100% ^2H_2O or 90% ^1H_2O/10% ^2H_2O (3−7 mM; 50 mM phosphate buffer, pH 6.2−7.8). Unless otherwise specified, all spectra were recorded at 298 K.

All ^{1}H NMR experiments were recorded on a Bruker AM 400/WB spectrometer equipped with an ASPECT 3000 computer at 400.13 MHz. Tailored acquisition parameters were used to remove base line distortions.[23] For 1D spectra, a sweep width of 11905 Hz was used to prevent spectral folding. The FID was collected with 8192 real data points resulting in an acquisition time of 0.69 s.

All homonuclear 2D spectra were acquired in the phase-sensitive mode, with sequential acquisition in the ω_2 dimension and quadrature detection in the ω_1 dimension achieved by TPPI:[24] ^{1}H DQF−COSY, TQF−COSY,[25] ROESY,[26] TOCSY,[27] and NOESY[28] spectra were generally recorded with spectral widths of 4950 Hz in both dimensions. This increased digital resolution in the diamagnetic spectral region at the expense of folding in the paramagnetic region. ^{1}H DQ−COSY experiments were carried out at three different DQ preparation periods (τ = 30, 60, and 90 ms) to maximize excitation for geminal (~14 Hz), vicinal (~7 Hz) and smaller couplings (~3 Hz). All 2D experiments were recorded with 384−768 ω_1 increments of 2048 real data points. Low power irradiation of residual water was normally required.

H−D exchange studies were carried out by exchanging ^1H_2O with ^2H_2O. Usually, 3−4 h was required to ensure complete solvent exchange, replacing all fast exchanging protons.[29] As a result, only nonlabile and slowly exchanging protons are observed in all spectra recorded and are referenced to the initially recorded spectrum (taken as t = 0 min). The H−D exchanged *Cp*Fd sample was characterized by a series of 1D and 2D spectra recorded over a period of 48 h.

For NOESY (50−250 ms) spectra, a 180° composite pulse placed in the middle of the mixing time was employed to prevent further relaxation recovery of the residual water peak.[30] Zero quantum coherences were not suppressed. TOCSY (40−80 ms) spectra were acquired in reverse mode using the MLEV-17 mixing scheme,[27] flanked by 500 μs trim pulses. ROESY spectra were recorded at 50 and 100 ms for both ^1H_2O and ^2H_2O samples and were obtained in Bruker

(18) Bloembergen, N.; Morgan, L. O. *J. Chem. Phys.* **1961**, *34*, 842.
(19) Sadek, M.; Scrofani, S. D. B.; Brownlee, R. T. C.; Wedd, A. G. *J. Chem. Soc., Chem. Commun.* **1995**, *1*, 105.
(20) Gaillard, J.; Moulis, J.-M.; Kümmerle, R.; Meyer, *Magn. Reson. Chem.* **1993**, *31*, S27.
(21) Rabinowitz, J. C. *Methods Enzymol.* **1972**, *24*, 431.
(22) Brereton, P. S.; Sadek, M.; Scrofani, S. D. B.; Brownlee, R. T. C.; Wedd, A. G. **1995**, Manuscript in preparation.
(23) Sadek, M.; Brownlee, R. T. C.; Scrofani, S. D. B.; Wedd, A. G. *J. Magn. Reson., Ser. B* **1993**, *101*, 309.
(24) Marion, D.; Wüthrich, K. *Biochem. Biophys. Res. Commun.* **1983**, *113*, 967.
(25) Rance, M.; Sørensen, O. W.; Bodenhausen, G.; Wagner, G.; Ernst, R. R.; Wüthrich, K. *Biochem. Biophys. Res. Commun.* **1983**, *117*, 458.
(26) Bax, A.; Davis, D. G. *J. Magn. Reson.* **1985**, *63*, 207.
(27) Bax, A.; Davis, D. G. *J. Magn. Reson.* **1985**, *65*, 355.
(28) Macura, S.; Ernst, R. R. *Mol. Phys.* **1980**, *41*, 95.
(29) Wüthrich, K. *NMR of Proteins and Nucleic Acids*; Wiley-Interscience Publications: New York, 1986.
(30) Brown, S. C.; Weber, P. L.; Mueller, L. *J. Magn. Reson.* **1988**, *77*, 166.

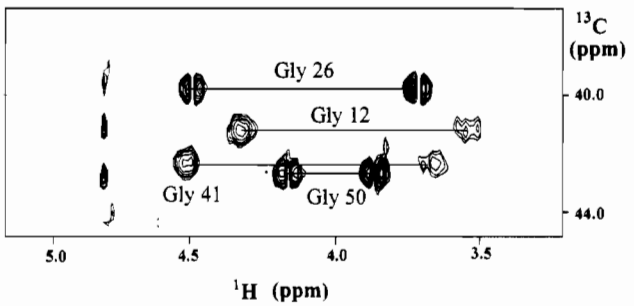

Figure 2. Partial 400-MHz {^{1}H−^{13}C}-HMQC spectrum of *Cp*Fd showing the (CH)$^{\alpha}$ region of the four Gly spin systems.

reverse mode with mixing achieved using small flip angle pulses of 20° and an effective spin-locking field of 3 kHz.[31]

{^{1}H−^{13}C}-HMQC spectra were recorded at natural abundance as described previously.[13] All ^{15}N experiments were recorded on ^{15}N labeled *Cp*Fd. Two-dimensional {^{15}N−^{1}H} INEPT experiments were acquired as described previously.[19] A {^{1}H−^{15}N}-HMQC−NOESY spectrum was recorded on a Bruker AMX500 spectrometer at the Biomolecular Research Institute, Melbourne, Australia, in the phase-sensitive mode with simultaneous acquisition in ω_2.[32] Spectral widths of 6024 and 5069 Hz were used in the ^{1}H and ^{15}N dimensions, respectively and an evolution period of 3 ms was utilized. A total of 4096 complex data points were collected with 512 t_1 increments and 96 transients per increment. The water signal was suppressed by low power irradiation for 100 ms during the relaxation delay and the mixing time. One dimensional ^{15}N spectra were recorded with gated decoupling to minimize NOE effects.

Data were processed on a SUN SPARCstation-2 using FELIX software (1.1) from Hare Research Inc. For spectral analysis, zero filling to 2048 real points in ω_1 was used. Windows were optimized iteratively for each 2D spectrum, however 60−80° shifted square sine bells were generally used in both dimensions, zero filled to form 2K × 2K real matrices. Proton chemical shifts were referenced to the $^{1}H_2O$ signal at 4.78 ppm (298 K), and ^{13}C chemical shifts were referenced indirectly to DSS in $^{1}H_2O$. ^{15}N resonances were referenced indirectly to $^{15}NH_4Cl$ (24.93 ppm, 2.9 M). $^{3}J_{NH\alpha}$ vicinal coupling constants were measured by the method of Kim and Prestegard.[33]

Results

Methods for Detection and Assignment of Resonances. The large variation in relaxation rates and hence line widths in this protein requires a much broader range of experiments than is normal for diamagnetic proteins. As well as the normal suite of 2D NMR experiments (DQF−COSY, TOCSY and NOESY) used to study low molecular weight proteins, a series of heteronuclear (HMQC and INEPT) and less commonly used ^{1}H COSY-type (DQ−COSY and TQF−COSY) experiments have been utilized. In addition, TOCSY[23] and NOESY[34] experiments, embodying shorter evolution times have been used to identify many of the faster relaxing nuclei present in *Cp*Fd.

Dispersion of broad and sharp resonances in crowded regions has resulted from the use of both directly and indirectly detected heteronuclear experiments. The {^{1}H−^{13}C}-HMQC experiment has been very effective in detecting a large number of paramagnetically affected resonances at natural ^{13}C abundance. For example, {^{1}H−^{13}C}-HMQC experiments have been used to identify almost all cysteinyl (CH)$^{\alpha}$ and (CH)$^{\beta}$ functions in clostridial ferredoxins.[12,13] This technique also readily identifies the four Gly spin systems present in *Cp*Fd (Figure 2) and shows that two of the four systems are broadened significantly, most likely due to paramagnetic effects (*vide infra*).

^{15}N detected NMR experiments have been utilized to identify **all** ^{15}N resonances in *Cp*Fd.[19] The ^{15}N detected 2D INEPT experiment has been found to be useful for identification of ^{15}N and, consequently, ^{1}H resonances of NH functions both remote from and close to the paramagnetic centers (Figure 3). In contrast, ^{1}H detected heteronuclear 2D NMR experiments (HMQC and HSQC) acquired under a variety of conditions have failed to detect a number of key NH groups.[19]

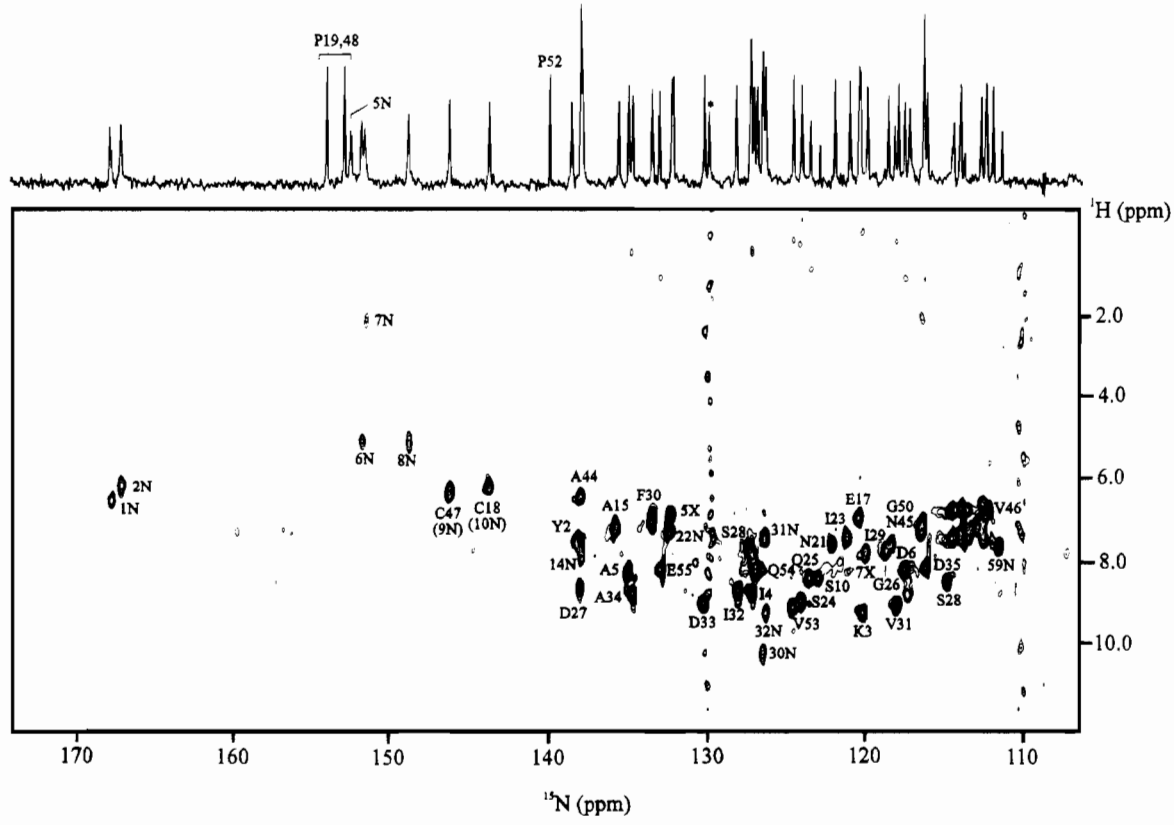

Figure 3. 400-MHz {^{15}N−^{1}H}-2D INEPT spectrum of *Cp*Fd. The ^{1}H decoupled 1D spectrum is also shown. The asterisk denotes an electronic spike.

In the present application, the DQ−COSY[35,36] experiment has been found to be a powerful tool for the identification of spin systems. One of the significant advantages of this technique over other COSY-type experiments is the unambiguous assignment of H^N-H^α cross peaks. Water presaturation effects do not interfere with detection of coupling between those H^α resonances located beneath or near the water resonance and their corresponding backbone amide protons.[37] In addition, remote and combination peaks allow unambiguous identification of spin systems, including those of magnetically equivalent species.[36,38,39] Seven of the eight Ala spin systems have been identified in DQ−COSY experiments by noting the presence of a remote peak indicative of the magnetic equivalence of $(CH_3)^\beta$ protons.

The TQF−COSY experiment in ^2H_2O is useful in helping to identify AMX-type residues, and residues with long side chains. For example, in *Cp*Fd, three of the four Gln/Glu spin systems exhibit unusually large separation between $H^{\beta,\beta'}$ resonances, attributable to paramagnetic shifting and/or aromatic ring current effects.

Spin systems were identified using the strategy developed by Chazin and Wright.[40] Backbone amide and terminal side chain proton resonances are used as initial points of assignment. The former feature a larger chemical shift dispersion compared to H^α resonances, are relatively isolated from other resonances (6−10 ppm), and are sensitive to pH and temperature changes. This fact can then be exploited to resolve overlapped spin systems. When no backbone amide proton resonance is observed, spin systems can normally be assigned to residue types through their characteristic resonance patterns.[29]

*Cp*Fd contains 55 amino acids (Figure 1), eight of which are cysteinyl ligands to the two Fe−S clusters. A total of 28 residues possess unique spin topology, (four Gly, eight Ala, one Thr, six Val, five Ile, one Lys, and three Pro), while there are 15 non-cysteinyl AMX-type spin systems (five Ser, five Asp, three Asn, one Tyr, one Phe). In addition, four nonunique longer-side chain residues are also present (two Glu, two Gln). Spin system assignments are presented in Table 1. Sequence-specific assignment of the cysteinyl H^α and H^β resonances has been described elsewhere.[12,13] Systems which could not be identified unambiguously due to a lack of connectivity are listed in Table 2.

Assessment of the Amide Fingerprint Region. ^1H DQ−COSY and TOCSY spectra acquired in ^1H_2O under a variety of conditions show the presence of about 80% of the expected H^N to H^α intraresidue connectivities. In contrast, one-dimensional ^{15}N ^1H-decoupled spectra of ^{15}N labeled *Cp*Fd detect all 61 possible ^{15}N resonances: 54 backbone, one Lys N^ζ, one N-terminal, and five carboxamide resonances. Two-dimensional ^{15}N detected INEPT experiments allow the corresponding ^1H amide chemical shifts associated with each ^{15}N resonance to be identified (Figure 3). All but one of the anticipated $^{15}N-^1H$ cross peaks have been detected.[19]

Sequence-Specific Resonance Assignments. The following section describes the sequential and long-range assignments made in *Cp*Fd using homonuclear and heteronuclear NOESY experiments. ROESY experiments were used to support these assignments and also to identify labile protons exchanging with solvent water. The unique Lys and Thr residues at positions 3 and 36, respectively (Figure 1) provide convenient sequence markers since they are on opposite sides of the molecule.[15] The amide fingerprint region of a 100 ms NOESY spectrum is shown in Figure 4, and sequential assignments are identified in Figure 5. Long-range NOE connectivities are presented in Figure 6.

Tyr 2 to Ser 7 Segment. A series of $d_{\alpha N}(i, i+1)$ connectivities are observed for the segment Tyr 2 to Ser 7. In addition, a number of NOE connectivities exist between Lys 3 side chain protons. A weak $d_{NN}(i, i+1)$ cross peak is observed between Asp 6 and Ser 7, and Ala 5 H^β resonance exhibits $d_{\beta N}$ connectivity with Ser 7 and a Gly spin system. Comparison with the *Cp*Fd structural model suggests that the most likely candidate for the latter is Gly 50.

Ala 15 to Glu 17 Segment. Spin systems Ala 15 and Ser 16 exhibit $d_{\alpha N}(i, i+1)$ and d_{NN} connectivities. This assignment is extended further to Glu 17 through the observation of a d_{NN} cross peak with Ser 16.

Ile 23 to Thr 36 Segment. Strong $d_{\alpha N}(i, i+1)$ and $d_{\beta N}(i, i+1)$ connectivities are observed for the unique Ser 24-Gln 25-Gly 26 segment. A weaker $d_{\gamma N}(i, i+1)$ connectivity is also observed between Gln 25 and Gly 26. A strong $d_{\alpha N}(i, i+1)$ cross peak involving Ser 24 H^N allows the identification of Ile 23. Both α-protons of Gly 26 show $d_{\alpha N}(i, i+1)$ connectivity with Asp 27 H^N. Although not apparent on spectra recorded at room temperature, NOESY spectra recorded at 287 K display $d_{\alpha N}(i, i+1)$ connectivity between Asp 27 and Ser 28. Weak $d_{\alpha N}(i, i+1)$ interactions are observed between Ser 28 and Ile 29, as well as strong d_{NN} (at 120 ms mixing time) and $d_{\beta N}$ connectivities.

Strong $d_{NN}(i, i+1)$ and $d_{\alpha N}(i, i+1)$ connectivities are observed for the unique tripeptide segment, Ala 34−Asp 35−Thr 36, where Asp 35 also exhibits $d_{N\beta}(i, i-1)$ and $d_{\beta N}(i, i+1)$ interactions in this segment. Specific assignment is extended further with the observation of $d_{\alpha N}(i, i+1)$ connectivities for the Ile 32−Asp 33−Ala 34 segment. Also observed is a weak NOE interaction between Asp 33 H^β and Ala 34 H^N. Ile 32 H^α exhibits $d_{N\alpha}(i, i-1)$ connectivity with the H^N resonance of one of two Val spin systems at 9.17 ppm. Spectra recorded at lower temperatures allow the Val systems to be distinguished and confirm $d_{\alpha N}(i, i+1)$ connectivity with Val $31^{H\alpha}$. $d_{N\alpha}(i, i-1)$ connectivity is also identified between Val 31 H^N and Phe 30 H^α. Strong d_{NN} connectivity is observed between Val 31 and Ser 24 and Gly 26 H^N exhibits NOE connectivities with both Phe 30 H^α and a Val 31 H^γ resonance.

Ala 44 to Val 46 Segment. Medium $d_{\alpha N}$, $d_{\beta N}$, and $d_{\alpha\gamma}$ connectivities allow the unique Asn 45−Val 46 segment to be assigned specifically. Strong $d_{\beta N}$ connectivity is observed between Asn 45 and an Ala spin system. The *Pa*Fd crystal structure[15] suggests that the adjacent residue Ala 44 is the only Ala residue close to Asn 45. The assignment of Ala 44 is confirmed through NOE cross peaks with Tyr 2 H^ϵ resonance in native and mutant forms of *Cp*Fd (*vide infra*). NOE cross peaks between the high field Val 46 $H^{\gamma,\gamma'}$ resonances and both H^β resonances of Glu 17 are also observed, as is a d_{NN} connectivity between Asn 45 and Glu 17.

Pro 52 to Glu 55 Segment. A $d_{\alpha N}$ connectivity within a Pro−Val segment is apparent. Although all three Pro residues in *Cp*Fd are part of such a sequence, an assignment Pro 52−Val 53 is possible as long-range NOE interactions between Val

(31) Kessler, H.; Griesinger, C.; Kerssebaum, R.; Wagner, K.; Ernst, R. R. *J. Am. Chem. Soc.* **1987**, *109*, 607.
(32) States, D. J.; Haberkorn, R. A.; Ruben, D. J. *J. Magn. Reson.* **1982**, *48*, 286.
(33) Kim, Y.; Prestegard, J. H. *J. Magn. Reson.* **1989**, *84*, 9.
(34) Busse, S. C.; La Mar, G. N.; Howard, J. B. *J. Biol. Chem.* **1991**, *266*, 23714.
(35) Bax, A.; Freeman, R.; Kempsell, S. P. *J. Am. Chem. Soc.* **1980**, *102*, 4851.
(36) Braunschweiler, L.; Bodenhausen, G.; Ernst, R. R. *Mol. Phys.* **1983**, *48*, 535.
(37) Otting, G.; Wüthrich, K. *J. Magn. Reson.* **1986**, *66*, 359.
(38) Bax, A.; Freeman, R.; Morris, G. *J. Magn. Reson.* **1981**, *42*, 164.
(39) Mareci, T. H.; Freeman, R. *J. Magn. Reson.* **1983**, *51*, 531.
(40) Chazin, W. J.; Wright, P. E. *Biopolymers*, **1987**, *26*, 973.

Table 1. Chemical Shifts of Amino Acid Residues for Oxidized Ferredoxin from *Clostridium pasteurianum*[a]

residue	NH	N	Hα	Cα	Hβ	H (other)	N (other)
Ala 1		39.0/40.8[b]	4.32	51.3	1.72		
Tyr 2	7.62	137.9	5.46	55.6	2.53, 2.79	Hδ 7.64; Hε 6.46	
Lys 3	9.35	120.1	4.78	53.0	1.88	Hγ 1.40; Hε 2.98, 2.92; HNζ 8.62	Nζ 39.0/40.8[b]
Ile 4	8.93	126.9	4.26	60.7	2.47	Hγ1 2.18; Hδ 1.73	
Ala 5	8.37	134.5	4.50	49.7	1.74		
Asp 6	8.32	117.4	4.38		2.87, 2.76		
Ser 7	7.25	112.7	4.29	55.2	3.86		
Cys 8			3.50		12.0,9.0		
Val 9			5.30	58.7	2.94	Hγ 1.34, 1.20	
Ser 10	8.50	122.6	4.40		3.88, 3.37		
Cys 11			10.0	98.1	15.8, 9.4		
Gly 12			4.29, 3.48	43.1			
Ala 13							
Cys 14	6.47/6.12[b]	166.8/165.2[b]	7.40	92.9	14.9, 4.9		
Ala 15	7.24	135.0	3.91	53.1	1.58		
Ser 16	7.78	126.9	4.45	56.9	4.03, 3.88		
Glu 17	7.01	120.2	4.40	52.6	2.08, 1.32	Hγ 1.82	
Cys 18	6.16	142.9	5.50		12.4, 6.2		
Pro 19	...	153.0/151.9[b]	5.17	63.0	2.90, 2.50	Hγ 3.04, 2.94	
Val 20	7.89	119.8	4.89		2.90	Hγ 1.07	
Asn 21	7.69	121.7	4.70	52.1	3.03, 2.72	HNδ 7.59, 7.13	Nδ 112.4
Ala 22							
Ile 23	7.54	120.8	5.08	58.9	1.63	Hγ1 1.42, 1.00; Hγ2 0.93	
Ser 24	9.07	123.8	4.66	54.2	3.73		
Gln 25	8.54	123.2	2.93	54.4	1.67, 1.20	Hγ 2.16; HNε 7.41, 6.68	Nε 112.4
Gly 26	7.83	118.4	4.45, 3.64	41.7			
Asp 27	8.54	137.4	4.37		2.71, 2.59		
Ser 28	8.62	114.5	4.39	56.9	3.91, 3.85		
Ile 29	7.69	118.0	4.60	58.4	Hγ 1.42, 1.00; Hδ 0.93		
Phe 30	7.07	133.0	4.95	56.8	2.70	Hδ 7.34; Hε 7.08, Hζ 7.20	
Val 31	9.17	117.8	4.50	57.3/58.9[b]	1.95	Hγ 0.91, 0.86	
Ile 32	8.83	127.8	4.69	58.9	2.47		
Asp 33	9.11	129.7	4.75	51.1	2.99, 2.65		
Ala 34	8.88	134.2	3.92	52.7	1.56		
Asp 35	8.21	115.9	4.52	53.9	2.77, 2.66		
Thr 36	7.33	114.0	4.26	60.1	3.90	Hγ 1.15	
Cys 37			3.3		11.2, 8.0		
Ile 38			5.13	59.1	2.56	Hγ2 1.04	
Asp 39					2.99, 2.86		
Cys 40			9.70	83.3	17.3, 9.3		
Gly 41			4.46, 3.57	44.3			
Asn 42					2.84, 2.69	HNδ 7.51, 6.84	Nδ 114.0
Cys 43	6.47/6.12[b]	166.8/165.2[b]	6.30	89.5	16.2, 5.0		
Ala 44	6.49	137.3	3.86	52.3	1.69		
Asn 45	7.36	116.2	4.46	52.7	2.80, 2.75	HNδ 7.56, 6.85	Nδ 114.4
Val 46	6.82	112.0	4.25	58.6	1.96	Hγ 0.56, 0.36	
Cys 47	6.34	145.4	4.5		13.6, 6.8		
Pro 48	...	153.0/151.9[b]	5.10	62.4	2.69, 2.36	Hγ 2.78, 2.57	
Val 49	7.98	128.4	4.99	57.7	2.86	Hγ 1.11	
Gly 50	7.15	116.2	4.11, 3.79	44.6			
Ala 51							
Pro 52	...	139.3	5.39	61.4	2.59, 2.24		
Val 53	9.18	124.3	4.50	57.3/58.9[b]	2.10	Hγ 0.98	
Gln 54	8.30	126.6	3.64	57.7	1.73, 1.17	Hγ 1.83, 2.08; HNε 6.68, 7.44	Nε 113.7
Glu 55	8.32	132.5	4.10	54.0	2.01, 1.92	Hγ 2.16	

[a] ^1H chemical shifts were referenced to the ^1H_2O signal at 4.78 ppm (298 K), and ^{13}C chemical shifts were referenced indirectly to DSS in ^1H_2O ppm. ^{15}N resonances were referenced indirectly to $^{15}NH_4Cl$ (24.93 ppm, 2.9 M). Proton chemical shifts are ± 0.02 ppm, nitrogen and carbon chemical shifts are ± 0.1 ppm. [b] Unambiguous assignment is not possible.

53 H^N and Lys 3 H^N are also apparent. The Pro 52 H^α resonance also shows strong NOE connectivity with Ile 4 H^α. {$^1H-^{15}N$}-HMQC–NOESY spectra exhibit strong NOE interactions between Val 53 H^α and Gln 54 H^N. A weaker connectivity is observed between Val 53 H^γ and Gln 54 H^N resonances. The assignment is extended further with the observation of a strong $d_{\alpha N}(i, i+1)$ connectivity between Gln 54 and Glu 55.

Both Gln 54 and Glu 55 have almost degenerate H^N resonances (8.30 and 8.32 ppm, respectively) in native *Cp*Fd, which makes the NOE cross peak with Tyr 2 H^α difficult to assign. However, {$^1H-^{15}N$}-HMQC–NOESY spectra show clearly that the NOE connectivity is between Tyr 2 H^α and Glu 55 H^N resonances. This long-range NOE interaction confirms the close spacial proximity of the terminal side chains.

Using the method of sequential and long-range assignments discussed above, the H^N and H^α resonances of 29 non-cysteinyl amino acid residues have been identified. Further advancement of assignments has required a combination of spectral techniques and selected mutants which are discussed below.

Extended Identification of Proline Spin Systems. Gaillard and co-workers have identified unambiguously the H^α and H^β resonances for Pro residues 19 and 48 from studies of mutant forms of *Cp*Fd.[11,20] {$^1H-^{13}C$}-HMQC spectra from the present work show that the H^γ resonances of both Pro 19 and Pro 48 overlap their respective H^β resonances. Although resonances

Table 2. Unidentified Spin Systems in Oxidized Ferredoxin from *Clostridium pasteurianum*[a]

system	type	NH	N	Hα	Cα	Hβ	H (other)
1X	Ala	8.00	126.7	3.77	50.7	1.46	
2X	Ala			4.27	53.3	1.39	
3X		8.79		4.07	59.3		
4X		6.93	131.7	4.29	53.2	2.00	1.26
5X		8.16		4.11	54.3		
6X		7.59	112.4				4.17; 5.17
7X	Ile						Hγ1 1.45, 1.20; Hδ 0.86
8X[b]							1.10
9X[b]							1.00
10X[b]							1.30
11X[b]							0.77
12X[b]							0.92
5N			151.5				
6N		5.03	150.9				
7N		2.17	150.7				
8N		5.13	148.0				
14N		7.84	137.4				
22N		7.30	131.6				
30N		10.27	126.2				
31N		7.49	126.1				
32N		9.20	125.9				
59N		7.72	111.4				

[a] Unidentified spin systems which exhibit at least side chain resonances are labeled X. Systems which only exhibit ^{15}N and/or ^{1}H resonances are labeled as N spin systems. Proton chemical shifts are ± 0.02 ppm; nitrogen and carbon chemical shifts are ± 0.1 ppm. [b] Spin systems which are likely to be part of either an Ile or Val side chain.

for Pro 52 $(CH_2)^{\gamma}$ and for the $(CH_2)^{\delta}$ functions of all Pro systems could not be detected, weak $d_{\beta\gamma}$ and $d_{\beta'\gamma}$ connectivities between Pro 48 and Val 49 are identified.

The ^{15}N resonances of the three proline residues are identified readily by comparing ^{1}H decoupled ^{15}N 1D spectra with INEPT and ^{1}H-coupled ^{15}N spectra. Two resonances fall very close to each other (153.0 and 151.9 ppm), while the third is at higher field (139.3 ppm) (Figure 3).[19] Noting this pattern and the fact that two of the three Pro residues in *Cp*Fd (Pro 19 and Pro 48) are related by a pseudo 2-fold axis of symmetry,[13] the highest field ^{15}N Pro resonance can be assigned to Pro 52. This then allows tentative assignment of the lowest field Pro resonances to Pro 19 and Pro 48, although specific assignment is not possible.

Specific Assignment of Glycine Spin Systems. *Cp*Fd possesses four Gly residues (Gly 12, Gly 26, Gly 41, and Gly 50). Mutant forms of *Cp*Fd have been produced where Gly 12 and Gly 41 (adjacent to Cys 11 and Cys 40, respectively) are either individually or both replaced by Ala.[13] DQF–COSY spectra of the single mutants (G12A and G41A) exhibit only three of the four Gly systems, allowing the absent system to be assigned specifically. $\{^{1}H-^{13}C\}$-HMQC spectra of native *Cp*Fd show that, although all four Gly residues possess very similar ^{1}H and ^{13}C chemical shifts, residues Gly 12 and Gly 41 are broadened significantly (Figure 2). Due to their close proximity to the Fe–S clusters, this broadening is likely to be due to paramagnetic effects. Analysis of the ^{1}H TOCSY and DQ–COSY spectra show that these two systems do not exhibit identifiable $H^{N}-H^{\alpha}$ cross peaks.

Aromatic Ring Resonances. Assignment of aromatic side chain ^{1}H resonances of the single Phe 30 residue has followed from DQF–COSY and TQF–COSY spectra recorded in $^{2}H_2O$, while assignment of Tyr 2 resonances was based on work by Packer and co-workers (*vide infra*).[41] Extension of ^{1}H assignments into the ^{13}C dimension was effected with $\{^{1}H-^{13}C\}$-HMQC spectra. No NOE interactions have been identified between ring protons and their corresponding β-protons, al-

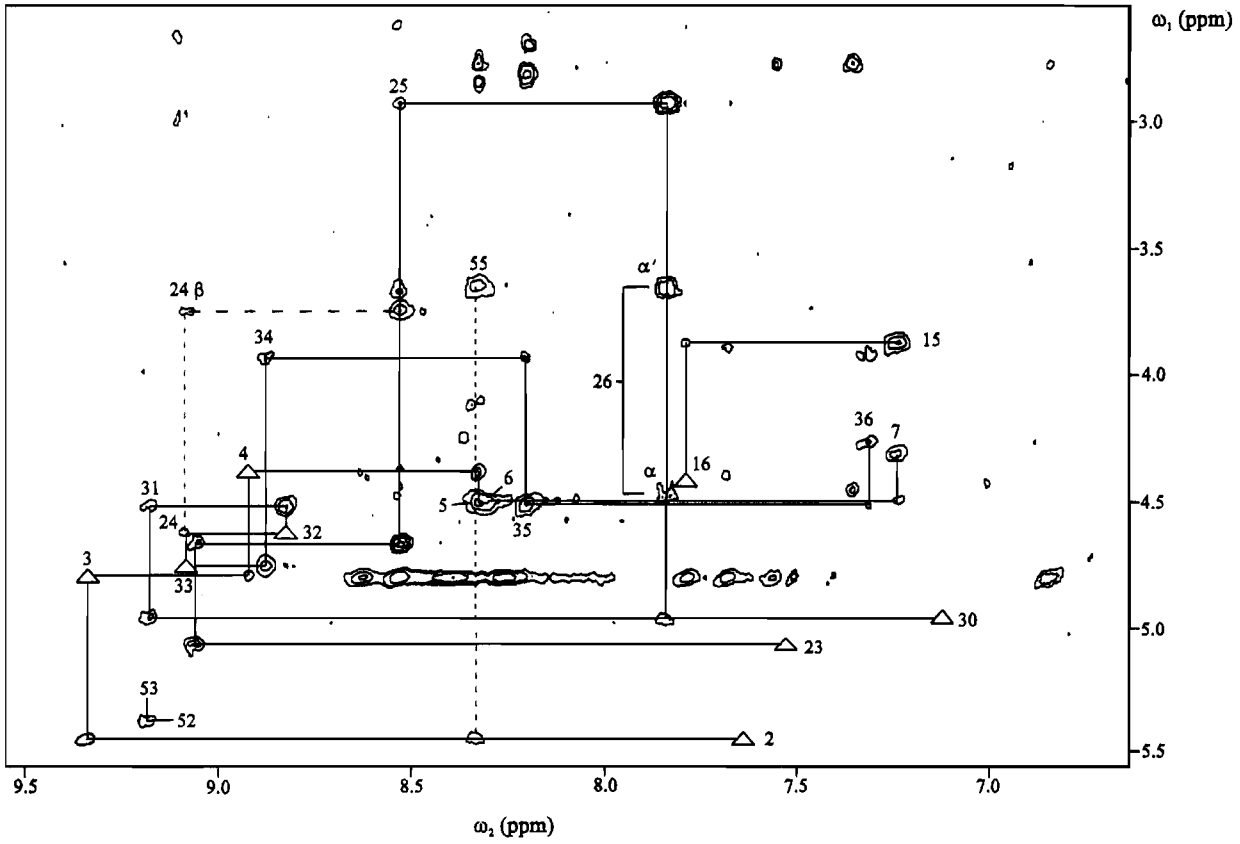

Figure 4. Fingerprint region of a 400-MHz NOESY spectrum of *Cp*Fd recorded with a 100 ms mixing time. Sequential $d_{\alpha N}$ connectivites are identified by the solid lines. Selected long-range NOEs are labeled with dashed lines.

Figure 5. Summary of sequential assignments H^{α}, H^{β}, and H^{N} resonances from 400-MHz NOESY spectra acquired with a 100 ms mixing time for *Cp*Fd. (a and b) Primary sequences of *Pa*Fd and *Cp*Fd, respectively, are shown. (c) Backbone amide protons that exchange slowly are indicated by a filled circle. (d) Identifiable $^3J_{NH\alpha}$ coupling constants greater than 7 Hz are labeled with open boxes, whereas coupling constants less than 7 Hz are labeled with a closed box. (e) The H^{α} chemical shifts are given relative to random-coil values for *Cp*Fd.[46] $\Delta\delta = \delta_{exp} - \delta_{random}$; Values greater than zero indicate shifts to lower field. Three or more consecutive residues with an index of +1 are indicative of a β-strand. The asterisks represent the paramagnetically affected cysteinyl residues. The CSI of Gln 25 cannot be defined due to significant shielding contribution to its chemical shift by Phe 30 aromatic ring. (f) Characteristic NOE connectivities ($d_{\alpha N}(i, i+1)$, $d_{\beta N}(i, i+1)$ and $d_{NN}(i, i+1)$) are depicted by the filled bars linking the two residues. The thickness of the bar relates to the intensity of the observable NOE connectivity at 100 ms mixing time.

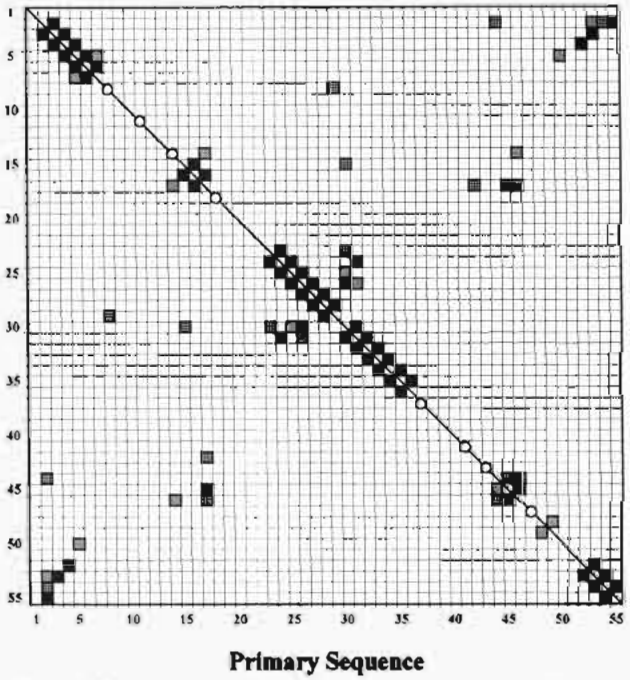

Figure 6. Diagonal plot of all NOE connectivities observed in *Cp*Fd at 100 ms, where both axes represent the primary sequence. NOE connectivities involving Cys residues presented previously[13] are also included. The filled boxes denote NOE connectivity between backbone protons (H^N or H^{α}) of the two residues in the sequence. Boxes with diagonal lines represent NOE connectivities between a backbone proton of one residue and a side chain proton(s) of another. Crosshatched boxes denote NOE connectivity between side chain protons of two separate residues. Circles indicate the positions of Cys residues. When more than one NOE connectivity is observed between two residues, only the stronger is shown.

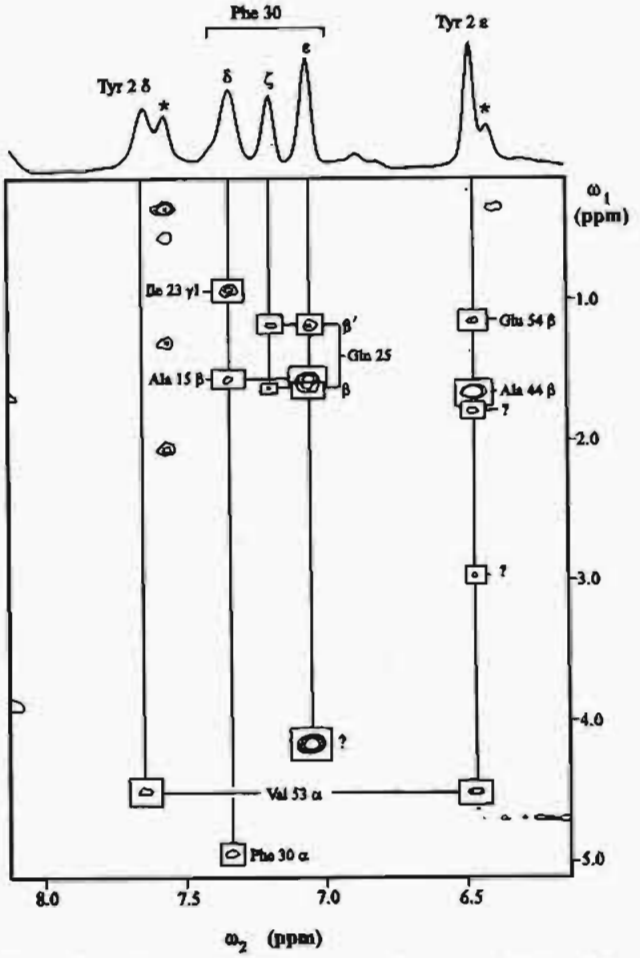

Figure 7. 400-MHz NOESY spectrum (50 ms) of *Cp*Fd in ^2H_2O recorded at 303 K, showing NOE connectivities with aromatic ring proton resonances. The resonances labeled with asterisks are due to cysteinyl protons. The resonances denoted by the question marks are yet to be assigned specifically.

though a NOE connectivity is observed between Phe 30 H^{δ} and H^{α} resonances (Figure 7).

NOESY spectra were recorded for ^2H_2O exchanged samples of native and mutant forms of *Cp*Fd in order to find possible NOE interactions with the aromatic rings of Tyr 2 and Phe 30. The NOESY spectrum of native *Cp*Fd demonstrates that Tyr 2 H^{ϵ} exhibits NOE cross peaks with at least five resonances (Figure 7), three of which are assignable to Val 53 H^{α}, Ala 44 H^{β}, and Gln 54 H^{β}. The remaining two cannot be assigned unambiguously due to overlap with other resonances in the aliphatic region. Val 53 H^{α} is also seen to possess NOE connectivity with the Tyr 2 H^{δ} resonance (Figure 7), as anticipated by the *Cp*Fd structural model which suggests that Val 53 H^{α} is less than 4 Å from the aromatic protons Tyr 2 $H^{\delta 2,\epsilon 2}$.

(41) Packer, E. L.; Sweeney, W. V.; Rabinowitz, J. C. *J. Biol. Chem.* **1977**, *252*, 2245.

Both Phe 30 H^{δ} and H^{ϵ} resonances possess NOE connectivities with Ala 15 H^{β}, as well as with Gln 25 $H^{\beta,\beta'}$. A NOE cross peak with Phe 30 H^{δ} is observed at 0.94 ppm; however, due to the large number of methyl proton resonances at or near this chemical shift, unambiguous assignment is not possible from the present data. Nevertheless, the most likely candidate is Ile 23 H^{γ}, since the structural model indicates that these protons are in close proximity to Phe 30 H^{δ}.

The most intense NOE connectivity in this region is observed between Phe 30 H^{ϵ} and a proton resonating at 4.17 ppm (spin system 6X: Table 2). However, this spin system cannot be assigned specifically.

Analysis of Carboxamide Groups. Homonuclear spectra show the presence of the five carboxamide groups expected for the Asn and Gln residues (Gln 25 and Gln 54, Asn 21, Asn 42 and Asn 45). The carboxamide protons of Gln 25 are assigned specifically through NOE interactions with their $H^{\beta,\gamma}$ protons. Strong NOE connectivities are identified between Glu 17 and carboxamide protons resonating at 7.51 and 6.84 ppm. Examination of the *Pa*Fd and *Cp*Fd structural models suggest that only the carboxamide group in close proximity to Glu 17 $H^{\beta,\gamma}$ is that of Asn 42. NOESY spectra of the G41A mutant show that the carboxamide ^1H resonances of both Asn 42 and an unidentified residue shift significantly upon mutation. Structural comparisons identify residues Asn 42 and Asn 45 as likely candidates. This observation consolidates assignment of Asn 42 $H^{N\delta,\delta'}$ and allows the further identification of Asn 45 $H^{N\delta,\delta'}$ resonances.

Two-dimensional NMR spectra of the D39N mutant demonstrate that Gln 54 has been affected (see supporting information). Of the two carboxamide groups which remain unassigned (Gln 54 and Asn 21), the proton resonances of only one are shifted in the D39N mutant. Since Asn 21 does not appear close to the site of mutation, the shifted resonances are assigned to Gln 54 $H^{\epsilon,\epsilon'}$.

Assessment of Assignments. A number of partially and fully identified spin systems cannot be assigned sequence-specifically using the above methods. These include one Ser, two AMX, four Ala, three Ile or Val (backbone and side chain), seven Ile or Val (side chain only) and four weak unidentified spin systems. However, there remain nine residues which have not had H^{α} resonances assigned using the above methods. They include one Ser (10), two Asn (21, 42), three Ala (13, 22, 51), two Val (9, 20) and a single Ile (38). A number of the missing residues can therefore be assigned by elimination. Since four of the five Ser spin systems have been assigned specifically, the remaining system is Ser 10. Asn 21 is assigned to one of the two remaining AMX spin systems by comparison with mutant spectra,[11,20] which allows the final system to be assigned specifically to Asn 42.

A series of mutant forms of *Cp*Fd have been designed to produce only minor perturbations to the local environment.[13,22] The D39N mutant has led to the assignment of the H^{β} resonances of residue 39, since they are the only unidentified AMX-type H^{β} resonances to be affected by the mutation (see supporting information). Crystallographic studies[14,42] suggest that a salt bridge between the carboxyl group of Asp 39 and the N-terminus of Ala 1 secures the N-terminal chain to the body of the protein. The H^{α} resonance of a single unidentified Ala spin system is also found to shift significantly (+0.17 ppm) in the D39N mutant. This system (which does not exhibit an identifiable H^{N} resonance in native or mutant forms) is consequently identified as the N-terminal residue, Ala 1. Difficulty remains in the identification of the three remaining Ala residues. Comparison with the *Cp*Fd structural model suggest that these residues are likely to be in close contact with the paramagnetic Fe−S clusters. As a consequence, NOE information used to make sequential assignments is likely to be lost due to increased relaxation rates.

*Cp*Fd possesses five Ile residues at positions 4, 23, 29, 32 and 38, and comparison with the *Pa*Fd crystal structure indicates that the side chains of a number of these residues will be less than 5 Å from an Fe−S center.[15] Backbone assignment of a number of Ile and Val spin systems has been hampered by a lack of some scalar connectivities in TOCSY- and COSY-type spectra.

In the D39N mutant, the H^{α} resonance of one of the three unassigned Ile/Val systems which exhibit H^{α} and H^{β} resonances shifts relative to native *Cp*Fd (+0.05 ppm). This is in contrast with the remaining two systems, where no perceived shifts are observed for any identifiable resonances. This system is assigned to Ile 38 since it is adjacent to the site of mutation. Mutation of the conserved Pro 19 residue in *Cp*Fd has resulted in shifts for the H^{β} resonance of a spin system attributed to Val 20.[43,44] This allows the the sequence-specific assignment of Val 9, which is well-removed from the site of mutation and close to cluster I.

The presence of more spin systems than can be accounted for suggests that either the protein possesses some flexibility or impurities are present in solution. The more likely case is the latter, since the purification of *Cp*Fd is alway accompanied by some protein degradation to the apo form.[45]

The results presented here show that 52 of the 55 amino acid residues in *Cp*Fd have been identified, with 86% of all protons being assigned.

Discussion

Assessment of Secondary Structure. Correlations between H^{α} chemical shifts and secondary structure have been identified.[46] H^{α} resonances in β-sheet structures tend to experience a downfield shift whereas the equivalent protons in α-helices shift to higher field. This method suggests that four or more consecutive residues with a chemical shift index (CSI) of +1 are indicative of a β-strand. Similarly, four or more consecutive residues with a CSI of −1 suggest an α-helical structure. However, *Cp*Fd exhibits many H^{α} resonances which are also likely to experience paramagnetic effects due to the $[Fe_4S_4]^{2+}$ centers, and so observed shifts cannot be taken to reflect solely the influence of secondary structure. Nevertheless, the use of shift data together with the observed long-range NOE connectivities allows prediction of the secondary structure in *Cp*Fd with some confidence.

Ala 5 H^{N}, which hydrogen bonds to Ala 50 CO in the *Pa*Fd crystal structure does not appear to exhibit a slowly exchanging H^{N} resonance in *Cp*Fd. However, the presence of a strong $d_{\beta N}(i, i+2)$ interaction between Ala 5 H^{β} and Ser 7 H^{N}, suggests that there is a turn in this region, which is supported by H^{α} shift indices of −1 for residues 6 and 7 and $^3J_{NH\alpha}$ coupling expected in type I/II turns (Figure 5).[29]

In *Pa*Fd, the cluster linking segments (residues 15−17 and 44−47) possess α-helical structure. The first segment (Lys 15−Pro 16−Glu 17) is notably different from that of *Cp*Fd (Ala

(42) Duée, E. D.; Fanchon, E.; Vicat, J.; Sieker, L. C.; Meyer, J.; Moulis, J.-M. *J. Mol. Biol.* **1994**, *243*, 683.
(43) Quinkal, I.; Davasse, V.; Gaillard, J.; Moulis, J.-M. *Protein Eng.* **1994**, *7*, 681.
(44) Gaillard, J. Personal communication.
(45) Moulis, J.-M.; Meyer, J. *Biochemistry* **1982**, *21*, 4762.
(46) Wishart, D. S.; Sykes, B. D.; Richards, F. M. *Biochemistry* **1992**, *31*, 1647.

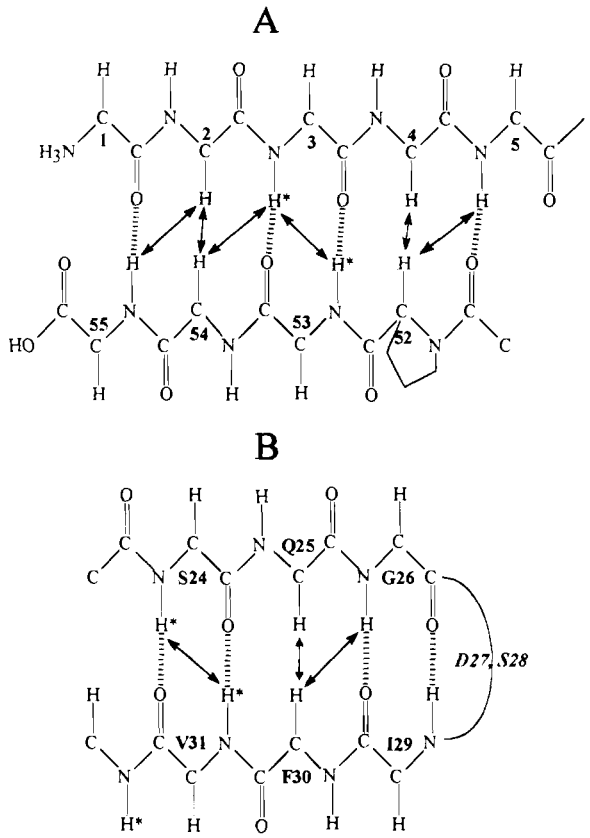

Figure 8. (a) NOE connectivities between terminal side chains indicating antiparallel β-sheet formation. (b) NOE connectivities in the major loop indicating which suggests antiparallel β-sheet structure. An asterisk denotes those residues which have been identified to possess slowly exchanging H^N resonances.

15−Ser 16−Glu 17), whereas the other cluster linking segments are very similar (*Cp*Fd, Ala 44−Asn 45−Val 46; *Pa*Fd, Ala 43−Ser 44−Val 45). Although the lack of long-range NOE information makes it difficult to confirm the structure in these segments, the results presented in Figure 5 suggest that these regions possess loosely defined helical structure.

The *Pa*Fd crystal structure suggests that the peptide segment between Cys 18 and Cys 37 forms a major loop in *Cp*Fd (Figure 1).[15] Preliminary analysis of the H^α shift indices in *Cp*Fd suggests the possibility of two β-strands (Figure 8). The pattern of NOE interactions indicates the presence of two separate antiparallel β-sheets, where segments Ala 1 to Ala 5 and Gly 50 to Glu 55 make up the first, and residues Ile 23 to Gly 26 and Ile 29 to Ile 32 identify the second. The pattern of NOE interactions and characteristic H^α chemical shifts in *Cp*Fd suggests that turns are present between residues Asp 27−Ser 28 and Asp 33−Thr 36 (Figure 8).

In *Cp*Fd, the major loop contains an extra residue at position 24 compared to *Pa*Fd. Consequently, the residues which are spacially close to the major loop in *Pa*Fd may be different to those in *Cp*Fd, a suggestion supported by ^{13}C NMR studies.[47] However, the NOE studies presented here show that the antiparallel β-sheet structure in the major loop of *Pa*Fd is retained in *Cp*Fd. The recenty published crystal structure of ferredoxin from *Clostridium acidi-urici* (*Cau*Fd; 73% homology)[42] also displays very similar structural characteristics to those described here for *Cp*Fd.

Amide Exchange Rates. Figure 5c lists slowly exchanging protons identified for *Cp*Fd. Slow solvent exchange is characteristic of amide protons involved in hydrogen-bonding interactions.[29] The amide proton region recorded approximately 6 months after dissolution in ^2H_2O (Figure 9a) exhibits at least 13 resonances, attributable to either cysteinyl or aromatic ring protons. Exchange experiments of *Cp*Fd freshly dissolved in ^2H_2O show that, while most amide protons have exchanged prior to the acquisition of the first 1D NMR spectrum (*ca.* 4 h—see Experimental Section), H^N resonances of Lys 3, Val 31, and Val 53 and an unidentified spin system (30N; Table 2) are still present after 24 h (Figure 9). Val 31 is the only residue with an observable H^N resonance after 48 h. The H^N resonances in the region 8.0−8.7 ppm exchange prior to the acquisition of the first spectrum and ROESY spectra show that these protons exchange with the solvent water.

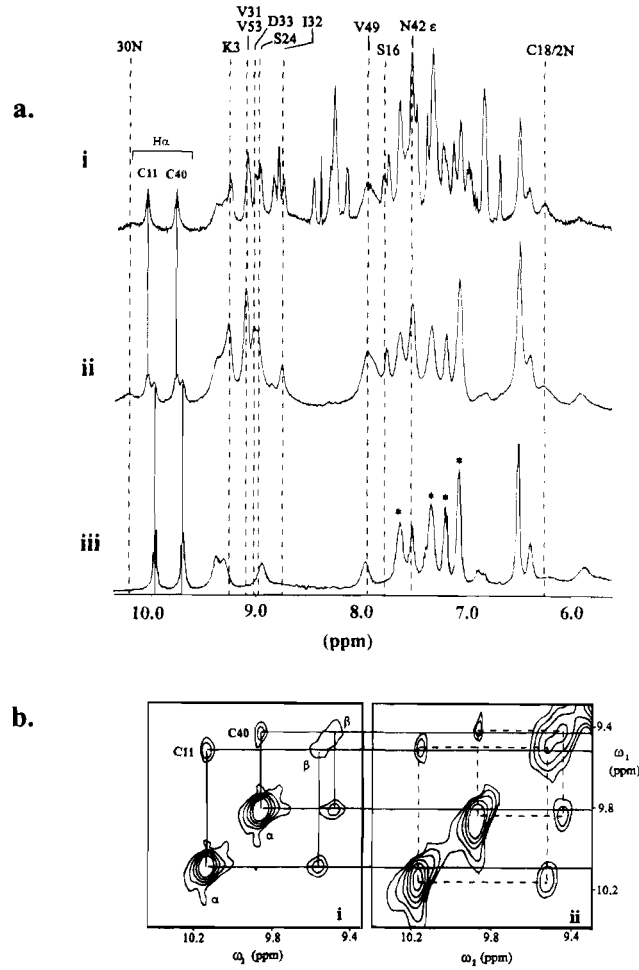

Figure 9. (a) Comparison of NH region under different solvent conditions. The 1D spectra were recorded in (**i**) ^1H_2O and (**ii**) $t = 0$ h and (**iii**) $t = 3$ months after dissolution in ^2H_2O. (b) TOCSY (40 ms) spectra showing Cys 11 and Cys 40 $H^\alpha-H^\beta$ connectivities in (**i**) ^2H_2O and (**ii**) ^1H_2O. The solid and dashed lines indicate relayed connectivities for these spin systems in ^2H_2O and ^1H_2O, respectively.

Four of the identified slowly exchanging resonances are due to residues which form part of the major loop (Ser 24, Val 31, Ile 32, and Asp 33), with a further two pertaining to the terminal side chains (Lys 3 and Val 53). Together with the previously described NOE connectivities for both sections, these results are highly suggestive of antiparallel β-sheet formation (Figure 8).

Effect of Amide Exchange Close to Cluster Sites. The rapid amide exchange observed by NMR techniques confirms observations made previously with other techniques. Electron spin resonance studies on *Cp*Fd demonstrated that the H−D exchange in the vicinity of the Fe−S clusters was significant

(47) Packer, E. L.; Rabinowitz, J. C.; Sternlicht, H. *J. Biol. Chem.* **1978**, *253*, 7722.

within 24 h.[48] Resonance Raman studies showed that the backbone amide protons involved in NH···S hydrogen bonding to cysteinyl and cluster sulfide atoms also undergo H−D exchange in ^2H_2O,[15] which suggests a high degree of solvent exposure for the Fe−S clusters.

^1H and ^{13}C NMR spectra suggest that symmetry-related residues Cys 11 and Cys 40 are strongly affected by paramagnetic interactions.[12,13] The α-protons of Cys 11 and Cys 40 appear to point *away* from the clusters[15] but both are located in regions where NH···S bonds to the active sites are highly concentrated (Figure 1). Although the H^α resonances of Cys 11 and Cys 40 are relatively sharp, they are located at about 10 ppm in the fully H−D exchanged spectrum of *Cp*Fd (Figure 9a). Interestingly, these same resonances are found at slightly lower field in ^1H_2O solution. The spectrum of a freshly H−D exchanged sample is presented in Figure 9a and shows the presence of four relatively sharp peaks which correspond to the resonances observed for both Cys 11 H^α and Cys 40 H^α in ^1H_2O and in fully H−D exchanged ^2H_2O spectra. A spectrum recorded after 4.5 h shows that the resonances corresponding to Cys 11 H^α and Cys 40 H^α in ^1H_2O have disappeared completely. TOCSY spectra recorded in ^1H_2O show the same cysteinyl H^α to H^β relayed connectivities as observed in ^2H_2O, although shifted (Figure 9b). The H^β resonances of these systems are also different for these solvents, although much less pronounced (< 0.03 ppm). It appears likely that H−D exchange at NH···S sites are affecting the nearby Cys 11 and Cys 40 H^α protons.

Aromatic Ring Effects. As described above (see Results), the assignment of Phe 30 ring protons was facilitated by the use of COSY-type spectra. Assignment of the Tyr 2 aromatic ring ^1H resonances in *Cp*Fd has been published.[49] However, these assignments are not consistent with the observations made in the present work. Pioneering deuterium labeling studies by Packer and co-workers[41] allowed the unambiguous assignment of tyrosine (Tyr 2 and Tyr 30) ring protons for ferredoxin from *Cau*Fd. A large relative shift was found between the H^δ and H^ϵ resonances for these residues (0.8 ppm) compared to that normally observed for aromatic rings in diamagnetic proteins (ca. 0.3 ppm).[50] Due to the high homology between the primary sequences of *Cau*Fd and *Cp*Fd (73% homology), resonances due to coupled protons which exhibit a similar relative shift in the aromatic region in *Cp*Fd are assigned to the sole tyrosine residue, Tyr 2. In support of this, NOESY spectra of the aromatic region show that, apart from resonances due to Phe 30 and cysteinyl protons, the only other resonances which exhibit observable NOE cross peaks are those which the present work assigns to the Tyr 2 ring protons (Figure 7). These NOE cross peaks are attributable to protons from residues in close proximity to Tyr 2 aromatic ring. In addition, {$^1H-^{13}C$}-HMQC spectra show intense $^1H-^{13}C$ cross peaks for aromatic ring proton resonances of Phe 30 and resonances assigned here to Tyr 2.

Hyperfine-Shifted ^{15}N Resonances. Crystallographic and resonance Raman studies have uncovered remarkable similarities in protein folding around the Fe_4S_4 clusters of a number of bacterial ferredoxins.[14,15,42,51] Each cluster features eight NH···S hydrogen bonds from peptide NH functions to cysteinyl S^γ or cluster sulfides. Figure 1 identifies the residues likely to be involved in such bonding.

Proton detected heteronuclear experiments are normally favored for protein studies due to their superior sensitivity. However, these methods are generally not useful for amide protons which relax quickly. In *Cp*Fd, only 39 of the possible 51 backbone amide protons have been identified by such techniques. Conversely, ^{15}N detected NH correlation experiments have identified all but one of these NH functions.[19] Interestingly, the NH functions which remain unassigned are just those identified as potential NH···S hydrogen bond donors (Table 1, Figure 1).

Disregarding the three Pro residues which possess ^{15}N resonances in the region between 140 and 170 ppm, there are eight resonances which are shifted to unusually low field (1N, 2N, 5N−10N: Figure 3). The symmetry relationship observed previously for paramagnetically affected ^1H and ^{13}C resonances[12,13] also appears to hold for these ^{15}N resonances.[19] Figure 3 shows seven $^{15}N-^1H$ cross peaks associated with these resonances, six of which can be paired in a similar fashion, allowing three symmetry-related pairs of amino acids to be identified (1N, 2N), (6N, 8N) and (9N, 10N). Resonance 7N has an uncharacteristically highfield ^1H chemical shift (2.17 ppm). The weak intensity of the cross peak suggests that it possesses a very short T_2/T_1 relaxation time.[19] Assuming the pairwise symmetry extends to H^N resonances, it appears likely that the unobserved H^N resonance associated with 5N would also be shifted to a similar region.

Although it is tempting to identify all eight low-field resonances as due to the eight cysteine residues, comparison with the *Pa*Fd crystal structure suggests that a series of non-cysteinyl residues possess amide functions in closer proximity to the clusters than a number of cysteines.[15] Recent studies on a ^{15}N-labeled reduced HiPIP have revealed ^{15}N resonances with shifts greater than 135.0 ppm.[10] These resonances have been assigned to non-cysteinyl residues involved in NH···S bonds with cluster sulfides.

The only paramagnetically affected resonances to be observed clearly *via* ^1H-detected 2D heteronuclear experiments are 9N and 10N. A homonuclear ^{15}N coupled TOCSY spectrum identifies H^N-H^α coupling for ^{15}N resonance 9N. Noting that only Cys 47 exhibits a H^α resonance at this chemical shift, this spin system is identified completely. Although no H^N-H^α cross peak is observed for the spin system associated with ^{15}N resonance 10N, it is assigned to Cys 18 through symmetry considerations. Consideration of the paramagnetic contribution to the chemical shift of ^{15}N nuclei can be used to make some tentative assignments for the remaining unassigned resonance pairs.

Markley and co-workers proposed that amino acid residues which are NH···S hydrogen donors to cluster sulfides are likely to experience both through-bond and through-space paramagnetic contributions to their chemical shifts and line widths.[5] The combination of these effects on so-called "class I" residues is likely to be more pronounced than those experienced by "class II" residues which experience pseudocontact effects only. Comparison with both the *Pa*Fd crystal structure and *Cp*Fd structural model suggest that a similar classification may hold for *Cp*Fd. The amide groups of symmetry-related residues Cys 14/43 are NH···S donors to cluster sulfides in *Pa*Fd.[15] Since these are the only cysteines which are likely to possess strong class I interactions, the two lowest field ^{15}N resonances (1N, 2N) may be assigned to Cys 14 and Cys 43. The remaining residues in close contact with the clusters are likely to possess varying degrees of paramagnetic contributions to their chemical

(48) Orme-Johnson, N. R.; Mims, W. B.; Orme-Johnson, W. H.; Bartsch, R. G.; Cusanovich, M. A.; Peisach, J. *Biochim. Biophys. Acta* **1983**, *748*, 68.
(49) Ganadu, M. L.; Bonomi, F.; Pagani, S.; Boelens, R. *Biochem. Int.* **1992**, *26*, 577.
(50) Gross, K.-H.; Kalbitzer, H. R. *J. Magn. Reson.* **1988**, *76*, 87.
(51) Adman, E. T.; Watenpaugh, K. D.; Jensen, L. H. *Proc. Natl. Acad. Sci. U.S.A.* **1975**, *72*, 4854.

shifts. Consequently, further assignments cannot be made with any certainty at this stage.

Conclusions

In the present work, 52 of the 55 amino acid residues in *Cp*Fd have been identified, with 86% of all protons being assigned. In addition, 38 of the 51 $(CH)^{\alpha}$ functions have been assigned unambiguously. The use of ^{15}N detected experiments on ^{15}N labeled *Cp*Fd has allowed regions very close to the paramagnetic centers to be probed, allowing all of the 61 ^{15}N resonances to be detected. Both ^{1}H and ^{15}N resonances for 35 of the 51 NH functions have been assigned unambiguously. Crystallographic studies[15,42] suggest that the nine non-cysteinyl residues for which the NH fragments remain unassigned are all likely NH···S hydrogen donors to either cysteinyl sulfur or cluster sulfides.

Protons less than 3 Å from the paramagnetic $[Fe_4S_4]^{2+}$ clusters can be observed successfully using the combination of NMR experiments described here. Work is currently underway using these assignments to probe electron transfer pathways in this protein. In addition, techniques to assign the remaining NH functions are being developed.

Acknowledgment. The authors acknowledge the Australian Research Council for financial support. Mr. P. S. Brereton is thanked for the preparation of mutant and native recombinant ferredoxins. Dr. R. S. Norton (Biomolecular Research Institute, Melbourne) is thanked for access to a Bruker AMX-500.

Supporting Information Available: Tables detailing the proton resonances affected by the G12A, G41A, G12,41A, and D39N mutants (2 pages). Ordering information is given on any current masthead page.

IC950116+